




Salmonella Facilitates Iron Acquisition through UMPylation of Ferric Uptake Regulator

Haihong Jia,^{a,b} Nannan Song,^{a,b} Yue Ma,^b Fengyu Zhang,^c Yingying Yue,^{a,b} Weiwei Wang,^{a,b} Cuiling Li,^{a,b} Hui Li,^b Qi Wang,^b  Lichuan Gu,^c  Bingqing Li^{a,b,d,e}

^aDepartment of Clinical Laboratory, Shandong Provincial Hospital Affiliated to Shandong First Medical University, Jinan, China

^bDepartment of Pathogen Biology, School of Basic Medicine, Shandong First Medical University & Shandong Academy of Medical Sciences, Jinan, China

^cState Key Laboratory of Microbial Technology, School of Life Sciences, Shandong University, Qingdao, China

^dKey Lab for Biotech-Drugs of National Health Commission, Jinan, China

^eKey Lab for Rare & Uncommon Diseases of Shandong Province, Jinan, China

Haihong Jia and Nannan Song contributed equally. These authors are listed in chronological order from the time they joined this study.

ABSTRACT Iron limitation is a universal strategy of host immunity during bacterial infection. However, the mechanisms by which pathogens antagonize host nutritional immunity have not been fully elucidated. Here, we identified a requirement for the UMPylator YdiU for this process in *Salmonella*. The expression of YdiU was dramatically induced by the metal starvation signal. The intracellular iron content was much lower in the $\Delta ydiU$ strain than in wild-type *Salmonella*, and the $\Delta ydiU$ strain exhibited severe growth defect under metal deficiency environments. Genome-wide expression analyses revealed significantly decreased expression of iron uptake genes in $\Delta ydiU$ strain compared with the wild-type strain. Interestingly, YdiU did not affect the expression level of the major iron uptake regulator Fur but directly UMPylated Fur on its H118 residue *in vivo* and *in vitro*. UMPylation destroyed the Fur dimer, promoted Fur aggregation, and eliminated the DNA-binding activity of Fur, thus abolishing the ability of Fur to inhibit iron uptake. Restricting Fur to the deUMPylated state dramatically eliminates *Salmonella* iron uptake in iron deficiency environments. In parallel, YdiU facilitates *Salmonella* survival within host cells by regulating the iron uptake pathway.

IMPORTANCE *Salmonella* is the major pathogen causing bacterial enteric illness in both humans and animals. Iron availability is strictly controlled upon *Salmonella* entry into host cells. The mechanisms by which *Salmonella* balances the acquisition of sufficient iron while preventing a toxic overload has not been fully understood. Here, we reveal a novel regulation process of iron acquisition mediated by the UMPylator YdiU. Fur acts as the central regulator of bacterial iron homeostasis. YdiU UMPylates Fur on H118 and prevents Fur from binding to target DNA, thus activating the expression of iron uptake genes under iron-deficient conditions. We describe the first posttranslational modification-based regulation of Fur and highlight a potential mechanism by which *Salmonella* can adapt to eliminate host nutritional immunity.

KEYWORDS Fur, *Salmonella*, UMPylation, YdiU, iron metabolism

Iron is an essential element for almost all living organisms. As a cofactor, the iron ion participates in multiple important life processes in bacteria, including nitrogen fixation, DNA synthesis, and damage repair (1, 2). Although iron is abundant in nature, the direct utilization of iron by organisms is difficult because of its poor solubility (3, 4). To prevent pathogenic bacteria from acquiring iron, host cells employ multiple strategies to limit the iron that is available for microorganisms in a process known as nutritional immunity (5–7).

Editor K. Heran Darwin, New York University School of Medicine

Copyright © 2022 Jia et al. This is an open-access article distributed under the terms of the [Creative Commons Attribution 4.0 International license](https://creativecommons.org/licenses/by/4.0/).

Address correspondence to Bingqing Li, bingqingsdu@163.com.

The authors declare no conflict of interest.

For a companion article on this topic, see <https://doi.org/10.1128/mbio.00207-22>.

Received 24 January 2022

Accepted 19 April 2022

Published 9 May 2022

To counter host nutritional immunity, bacteria have evolved multiple approaches to acquire sufficient iron from their hosts and other iron-deficient environments. The synthesis of enterobactin (Ent), a catechol siderophore with high iron affinity, is a main survival strategy in *Enterobacteriaceae* species, including *Escherichia coli*, *Salmonella enterica* serovar Typhimurium, and *Klebsiella pneumoniae* under iron-deficient conditions (8–11). Ent is assembled by the nonribosomal peptide synthetase (NRPS) composed of EntB, EntE, and EntF proteins (12). Synthesized Ent is secreted out of the cell to capture iron atoms. Fe-bound Ent is then recognized and transported into the cytoplasm by a series of ferric-enterobactin uptake proteins (FepABCDEG) (13). Intriguingly, although iron is necessary, it is harmful to bacteria at high concentration. The Fenton reaction will occur in the presence of a high concentration of intracellular iron and H₂O₂, producing a large number of hydroxyl radicals that subsequently lead to macromolecular damage and bacterial death (14). Thus, iron is required to be at an appropriate level so bacteria can obtain needed iron but also avoid excessive iron-induced damage.

The highly conserved gene *fur* (ferric uptake regulator) is the major regulator of iron homeostasis in bacteria (15–17). When iron ions are abundant, Fe-Fur binds the promoters of iron uptake-related genes, interfering with RNA polymerase binding to block transcription of these genes (18, 19). When bacteria move from an iron-rich environment to an iron-deficient environment (such as inside host cells), the transcription of iron uptake genes can restart (20–22). Lee et al. proposed a Fur working model in which a small amount of intracellular iron results in the release of iron ions from Fur and Fur free from Fe²⁺ releases from the DNA, allowing RNA polymerase to bind the promoters and transcribe the iron uptake (18). However, there are uncertainties in this widely accepted mechanism. For example, in *Campylobacter jejuni*, Fur forms dimers and binds the promoter regions of target genes even in the absence of the iron cofactor (23). In addition, metal-unbound mutants of *Bradyrhizobium japonicum* Fur still repressed gene expression *in vivo* (24). More importantly, *in vitro* studies have shown that in addition to iron, Fur can bind manganese and cobalt ions to achieve high DNA binding activity (18, 25), suggesting that Fur regulation is more complex than strict iron dependence. A protein named EIIA was reported to directly interact with Fur and regulate its DNA binding activity (26). Recently, we reported that YdiV, the flagellar regulatory protein, can change the conformation of Fur with the assistance of the chaperone SlyD during the folding of Fur, interfering with its DNA binding activity (27).

Protein posttranslational modification is an important way to regulate protein function, but modification of Fur has not been reported. We previously identified a ubiquitous and highly conserved protein, YdiU, as an enzyme that catalyzes UMPylation, modifying bacterial proteins with UMP (28). Mass spectrometry-based proteomic analysis identified 46 UMPylated bacterial proteins in the YdiU-expressing *Salmonella* strain, including Fur (28). However, the function of YdiU after induction during iron deficiency and the potential effects of YdiU on Fur remain unclear.

Previous studies suggested a relationship between YdiU and bacterial iron metabolism. First, the expression of YdiU was reported to be regulated by an iron signal-related transcription factor, IcsR (29, 30). In an *iscA sufA* mutant strain lacking iron-sulfur clusters and known iron uptake-related genes, the expression of YdiU is dramatically upregulated 8.3-fold (31). Domain analysis of the genomes from multiple species revealed that *fur* and *ydiU* genes are located in close proximity, increasing the probability of coordinated expression and suggesting an association between YdiU and Fur (32). Given that Fur can be UMPylated in YdiU-expressing *Salmonella*, we proposed that YdiU can modify Fur via UMPylation to regulate iron uptake in bacteria when iron was limited.

The experiments performed in this study support the above-described hypothesis. First, we confirmed that YdiU could be effectively induced by metal deficiency. Next, we found that, compared with the wild-type strain, the *ydiU* mutant strain exhibited significantly reduced viability and significantly decreased intracellular content of iron under metal-deficient conditions. Proteomics data revealed that expression of genes related to Ent biogenesis and acquisition significantly decreased in the $\Delta ydiU$ cells with no obvious difference in Fur expression levels, indicating that the regulation of iron uptake-related genes by YdiU occurred after translation of Fur. More importantly, we found that YdiU catalyzed UMPylation of Fur both *in*

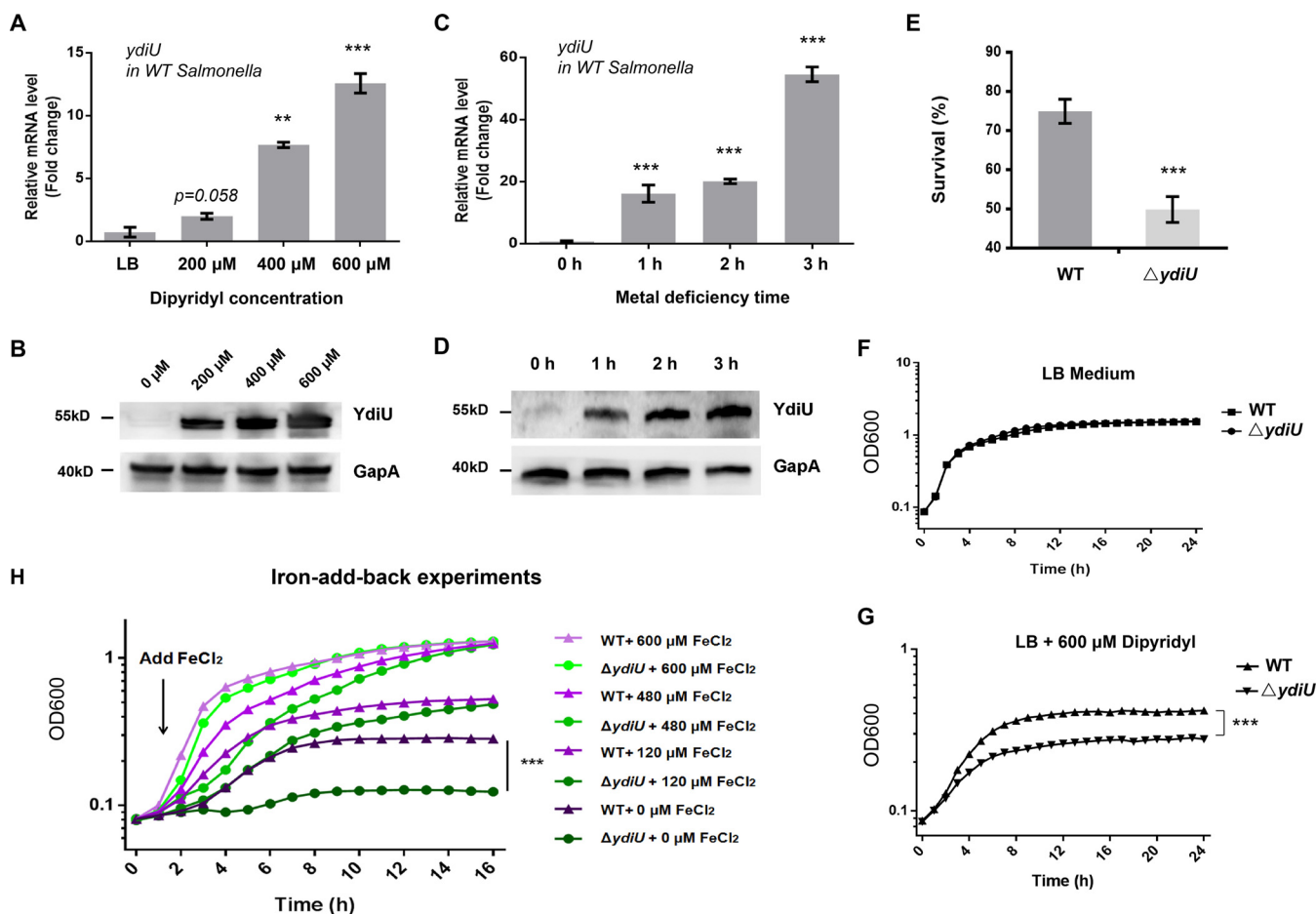


FIG 1 YdiU is involved in the iron metabolism pathway. (A and B) The transcription and protein levels of YdiU in *Salmonella* cultivated with different concentrations of 2,2'-dipyridyl were detected with qRT-PCR and Western blotting, respectively. GapA (also known as glyceraldehyde-3-phosphate dehydrogenase [GAPDH]) was used as a loading control. (C and D) The transcription and protein levels of YdiU in *Salmonella* treated with 600 μ M 2,2'-dipyridyl for the indicated times were detected with qRT-PCR and Western blotting, respectively. (E) The survival rates of WT and $\Delta ydiU$ strains after metal deprivation for 3 h. (F and G) The growth curves of WT and $\Delta ydiU$ cultivated in LB medium or metal-limited medium. (H) Iron add-back experiments of wild-type and $\Delta ydiU$ cells. Different concentration of $FeCl_2$ was added into the corresponding cultures 2 h after metal ion deprivation. The above-described experiments were performed as three replicates, and the mean values are presented. ***, $P < 0.001$; **, $P < 0.01$; *, $P < 0.05$ compared with the WT strain cultivated in LB medium (A and C) or with the WT strain under identical conditions (E).

in vivo and *in vitro*. UMPylation destroyed Fur dimers and made Fur more likely to aggregate. Moreover, the UMPylated Fur lost its DNA binding activity. The regulation of iron uptake by YdiU was independent of its upstream gene *ydiV* but dependent on *fur* and UMPylation activity. The results of *in vivo* experiments indicated that the YdiU-mediated regulation of iron uptake is critical for *Salmonella* survival for cells experiencing iron deficiency. Overall, we revealed a mechanism by which posttranslational modification can regulate Fur function and effectively initiate bacterial iron uptake, facilitating *Salmonella* survival within host cells.

RESULTS

YdiU is involved in the iron metabolism pathway of *Salmonella*. Our previous data showed that YdiU was expressed at a very low level when *Salmonella* was cultured in Luria-Bertani (LB) medium but strongly induced when metal-chelating agent 2,2'-dipyridyl was added (28). Dipyridyl is a metal chelator that binds nickel, cobalt, iron, and zinc with almost equal affinity. To further investigate the correlation between metal starvation and YdiU expression, the mRNA and protein levels of YdiU were measured for *Salmonella* cultured in LB medium supplemented with different concentrations of dipyriddy. Our data showed that the expression of YdiU was efficiently induced by dipyriddy, and expression increased with increased dipyriddy concentration (Fig. 1A and B). The real-time expression

of YdiU was determined 1 h, 2 h, or 3 h after the addition of dipyriddy. The results indicated that YdiU was expressed 1 h after metal starvation and continued to increase with increased time (Fig. 1C and D). Specifically, when cells were incubated with dipyriddy for 1, 2, and 3 h, the mRNA level of *ydiU* increased 16.2-, 19.8-, and 54.6-fold, respectively (Fig. 1C), and protein levels of YdiU increased 14.5-, 23.7-, and 44.2-fold, respectively (Fig. 1D). These data demonstrate that the metal starvation signal dramatically induced YdiU expression.

To explore the function of YdiU in metal homeostasis, cell survival was monitored using wild-type (WT) and $\Delta ydiU$ *Salmonella* grown under metal-limited conditions. The survival rate of WT cells was 74.94% in metal-deprived medium, but the survival rate of the $\Delta ydiU$ strain was only 49.78% under the same conditions (Fig. 1E). Importantly, although the growth curves of WT and $\Delta ydiU$ strains were similar in LB medium, $\Delta ydiU$ cells cultured in metal-deprived medium grew significantly differently than WT cells, with the optical density at 600 nm (OD_{600}) value of WT cells reaching a plateau of about 0.41 but $\Delta ydiU$ cells reaching only 0.25 (Fig. 1F and G). The metal add-back experiments then were performed. The result showed that the addition of iron rescues the growth defect of $\Delta ydiU$ *Salmonella* under metal deficiency conditions in a dose-dependent manner (Fig. 1H). Iron rescues growth defect, but an influence of other metals cannot be fully excluded.

YdiU facilitates iron absorption by activating iron uptake gene transcription.

To further clarify the function of YdiU, mass spectrometry-based proteomics were used to analyze the differences in global protein expression in WT and $\Delta ydiU$ cells grown with dipyriddy (see Fig. S1 in the supplemental material). Overall, a total of 251 proteins were found to be differentially expressed when the *ydiU* gene was deleted, with fold change of $>30\%$ and *P* value of <0.01 , of which 113 genes were upregulated and 138 genes were downregulated. These proteins fall into several categories, including cell motility, iron homeostasis, virulence, and energy production. Because our focus is on the function of YdiU on iron metabolism, we next analyzed genes related to iron metabolism. Interestingly, several iron uptake-related proteins were significantly repressed in $\Delta ydiU$ strain (Fig. 2A to C). Remarkably, the enterobactin biosynthesis proteins (EntABCDEF) and ferric-enterobactin uptake proteins (FepABCDEG) were all reduced to $\sim 50\%$ in $\Delta ydiU$ strain compared with the WT strain. Synthesis of enterobactin is a major strategy that *Salmonella* uses to salvage iron within host cells and under other iron-limited conditions (Fig. 2D) (9, 33, 34), so we hypothesized that YdiU facilitates iron absorption by increasing the levels of proteins involved in enterobactin biosynthesis and ferric-enterobactin uptake. The altered expression of iron uptake genes was confirmed using quantitative PCR (qPCR) by representative genes *entE* and *fepA*. The expression levels of *entE* and *fepA* in the $\Delta ydiU$ strain dropped to 20% to 50% of the levels in the WT strain under metal-deficient conditions (Fig. 2E and F). The complementation of *ydiU* in the $\Delta ydiU$ strain restores the expression levels of these genes, confirming this effect is due to the requirement of YdiU (Fig. S2). Compared with the $\Delta ydiU$ strain, the transcription of *entE* and *fepA* genes in the *ydiU* strain showed dramatic increases under metal-deficient conditions, 21.44-fold for *entE* and 3.5-fold for *fepA* (Fig. S2B and C). To further investigate the role of YdiU in iron absorption, we measured the intracellular iron concentrations in the WT and $\Delta ydiU$ strains by inductively coupled plasma mass spectrometry (ICP-MS) in LB and metal-deficient medium. Interestingly, there was no significant difference in the cellular iron concentration in the WT and $\Delta ydiU$ strains under iron-rich conditions (Fig. 2G). However, in metal-deficient medium, the intracellular iron concentration of $\Delta ydiU$ strain was significantly reduced to $\sim 60\%$ of that in the WT strain, with an average of 572.7 pmol/mg cells in the WT strain and 340.1 pmol/mg cells in *ydiU* mutant strains (Fig. 2H). These data demonstrate that YdiU acts as an activator for iron uptake by upregulating the transcription of iron uptake genes.

Neither *fur* mRNA nor Fur protein level is affected by YdiU. The iron uptake pathway is mainly controlled by Fur in *Salmonella* (35). Previous transcriptomics data demonstrated that the expression of the *fur* gene is at a high level when *Salmonella* organisms enter host cells, and expression of iron uptake genes increases 10- to 20-fold after *Salmonella* organisms enter host cells (36, 37). The strategy by which *Salmonella* can relieve the inhibitory effect of Fur to activate iron uptake genes has not been fully elucidated. Our proteomic data revealed no obvious difference at the protein level of Fur between WT and $\Delta ydiU$ strains under metal-deficient conditions (Fig. S3A). Next, qRT-PCR was used to evaluate a potential effect of YdiU

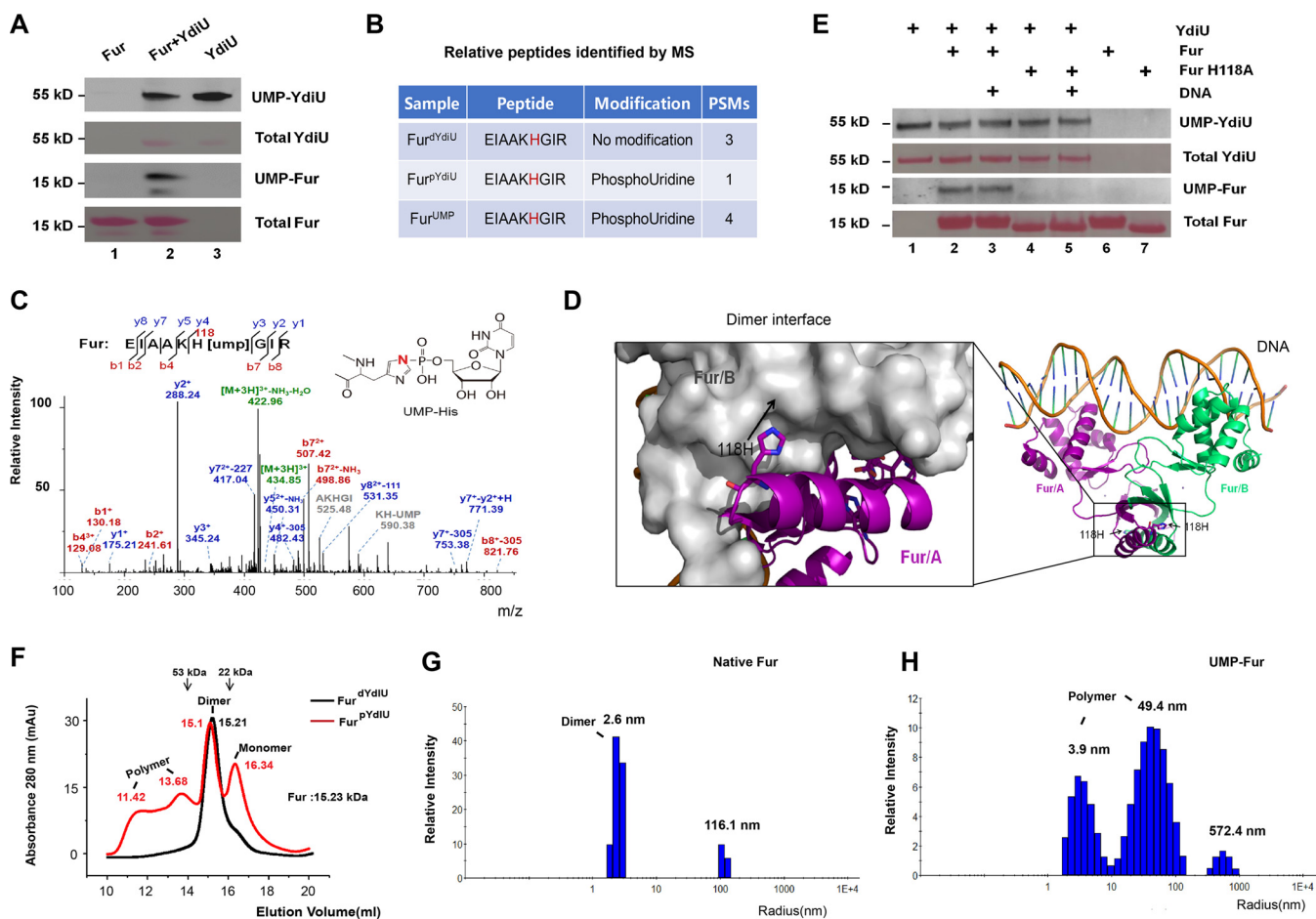


FIG 3 UMPylation of Fur by YdiU at H118 alters Fur's aggregation state. (A) *In vitro* UMPylation of Fur catalyzed by YdiU. UMPylation reaction mixtures were performed with biotin-16-UTP and $MnCl_2$, followed by avidin blotting. Total proteins were visualized by Ponceau S staining. (B) UMPylated peptides of Fur identified by mass spectrometry in Fur^{dYdiU}, Fur^{pYdiU}, and Fur^{UMP}. (C) Electrospray ionization tandem mass spectrometry (MS/MS) spectra of UMPylated peptides identified in Fur^{UMP}. The b and y ions are indicated along the peptide sequence above the spectra. Unique ions (111.1, 227.1, and 305.1 Da) corresponding to the neutral loss of the UMP group were detected in the MS/MS spectra of UMPylated peptides. (D) Structural presentation shows that H118 is located in the dimeric interface. H118 is highlighted in stick form. Shown is PDB entry 4RB3. (E) *In vitro* UMPylation of native Fur and FurH118A in the absence and the presence of excess DNA. The UMPylation reactions were performed with biotin-16-UTP and $MnCl_2$, followed by avidin blotting. Total proteins were visualized by Ponceau S staining. (F) Size-exclusion chromatography (SEC) results of Fur^{dYdiU} and Fur^{pYdiU}. The elution volume of each peak value is indicated in the corresponding colors. (G and H) The characteristics of native Fur and UMPylated Fur were determined by dynamic light scattering. Both YdiU and Fur proteins used in the above-described experiments were from *E. coli*.

detected, but H118 was identified as a novel UMPylation site. Further, UMPylation on Fur H118 was detected in Fur^{pYdiU} and Fur^{UMP} but not in Fur^{dYdiU}, demonstrating H118 acts as an UMPylation site both *in vitro* and *in vivo* (Fig. 3B and C).

The UMPylated sites are located in positions of Fur essential for dimerization and iron binding. To investigate the effect of UMPylation on Fur, we analyzed the spatial structure of UMPylation sites H33 and H118. H33 is located near the iron-binding site (Fig. S4B). In the apo-Fur structure, H33 is relatively exposed, but in holo-Fur, H33 is coordinated with manganese (19). Thus, UMPylation of Fur by YdiU might be regulated by the binding state of Fur, where UMPylation of H33 might be favored for the iron-unbound form of Fur. Residue H118 was also detected as a site of UMPylation both *in vivo* and *in vitro* (Fig. 3B and C), and this residue is located on the surface of the Fur homodimer (Fig. 3D). The addition of UMP moiety to H118 could disrupt the dimer interface and thereby alter the protein aggregation state of Fur. By sequence alignment, we found that these UMPylated residues (H33 and H118) are highly conserved across Fur's orthologs, suggesting the regulation of Fur by YdiU-mediated UMPylation is employed widely (Fig. S6). The H118A mutant of Fur could not be UMPylated by YdiU, confirming H118 was the major UMPylated site of Fur *in vitro* (Fig. 3E).

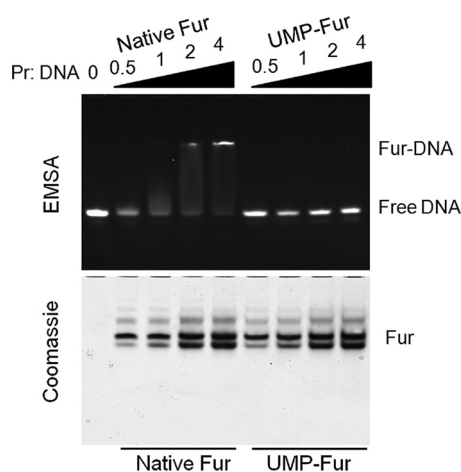


FIG 4 UMPylation prevents Fur from binding target DNA. Electrophoretic mobility shift assays (EMSAs) were performed for native Fur and UMPylated Fur with Fur box DNA. In these assays, 10 nmol FAM-labeled Fur box DNA was mixed with 0 to 40 nmol native Fur or UMPylated Fur for 10 min at 30°C and then analyzed by EMSA. The upper and lower pictures show the same gel imaged by fluorescence or stained with Coomassie brilliant blue. The experiment was repeated three times with similar results. Fur used in the above-described experiments was from *E. coli*.

The UMPylated Fur presents a different aggregation state with native Fur. To further investigate the effect of UMPylation on the characteristics of Fur, we analyzed Fur^{dYdiU} and Fur^{pYdiU} using size exclusion chromatography (Fig. 3F). Fur^{dYdiU} exhibited a single elution peak at 15.21 mL, implying that Fur forms a homodimer without UMPylation. Interestingly, Fur^{pYdiU} showed a more complex result, with four major elution peaks (11.42 mL, 13.68 mL, 15.1 mL, and 16.34 mL), demonstrating a changed aggregation state of Fur after YdiU-mediated UMPylation. The elution peak at 16.34 mL shows that UMPylation split the Fur dimer into the Fur monomer form. The peaks at 11.42 mL and 13.68 mL suggest that UMPylation converts Fur to an aggregation-prone state. *In vitro* UMPylation was performed using Fur^{dYdiU} and YdiU to obtain fully UMPylated Fur (Fur^{UMP}), and the characteristics of native Fur and Fur^{UMP} were compared using native gel and dynamic light scattering (DLS). The bands of Fur^{UMP} are shifted compared with those of native Fur (Fig. S7). Large polymers with an ~49.4-nm radius were produced after UMPylation, as detected by dynamic light scattering (Fig. 3G and H). All these results showed that Fur became less stable and more aggregated after UMPylation.

UMPylation impaired the DNA-binding activity of Fur. Fur inhibits the transcription of iron uptake genes by directly interacting with promoter DNA (39, 40). The DNA binding ability of native Fur and UMPylated Fur was compared using electrophoretic mobility shift assay (EMSA) and using different molar ratios of Fur and DNA. A clear DNA shift was detected for a molar ratio of native Fur and DNA greater than 1; however, no shift was detected using UMPylated Fur even at a ratio of protein and DNA greater than 4 (Fig. 4). The complete loss of DNA binding activity by UMPylated Fur suggests that YdiU regulates the iron uptake pathway by UMPylating and inactivating Fur.

Regulation of iron uptake by YdiU depended on Fur and UMPylation activity. A YdiU D248A mutant *Salmonella* strain was constructed as a strain in which YdiU lacks UMPylation activity (28). Comparing the wild-type and D248A mutant strains, we found that the expression of iron uptake genes in mutant bacteria was significantly decreased compared to that in wild-type bacteria under iron-deficient conditions, indicating that the regulation of iron uptake by YdiU was dependent on its UMPylation activity (Fig. 5A). To further explore the effect of YdiU on iron uptake, a vector allowing strong and constitutive expression of the *ydiU* gene was constructed and transformed into WT, $\Delta ydiU$, and Δfur strains (WT *pydiU*, $\Delta ydiU$ *pydiU*, and Δfur *pydiU* strains, respectively). The expression levels of *entE* and *fepA* were determined by qPCR for the original strains and YdiU-expressing strains under the iron-deficient condition (Fig. 5B to D). The plasmid-driven expression of YdiU in the WT and $\Delta ydiU$ strains dramatically increased the expression of iron uptake genes; however, in

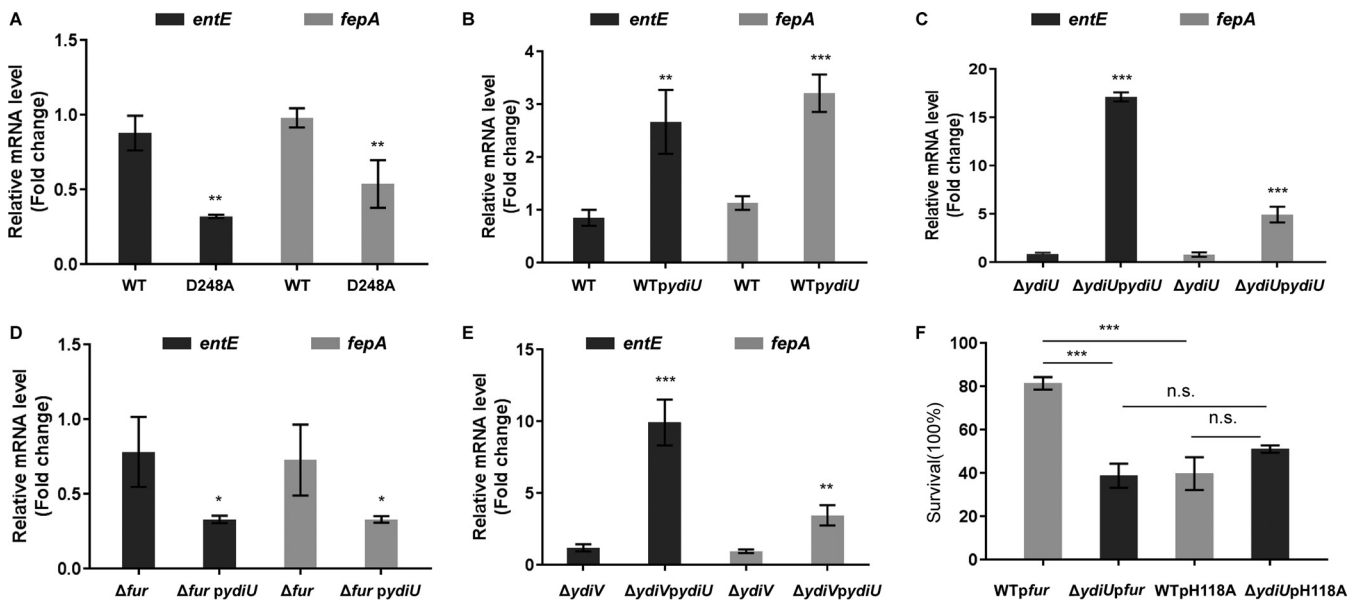


FIG 5 Regulation of iron uptake by YdiU is dependent on the UMPylation activity and Fur. (A to E) The transcription levels of iron uptake genes (*entE* and *fepA*) in *Salmonella* strains cultured under iron deficiency conditions were detected by qRT-PCR. (A) The mRNA level of *entE* and *fepA* in WT and YdiU D248A mutant strains. (B) The mRNA level of *entE* and *fepA* in WT and WT pYdiU strains. (C) The mRNA level of *entE* and *fepA* in $\Delta ydiU$ and $\Delta ydiU$ pydiU strains. (D) The mRNA level of *entE* and *fepA* in Δfur and Δfur pydiU strains. (E) The mRNA level of *entE* and *fepA* in $\Delta ydiV$ and $\Delta ydiV$ pydiU strains. (F) The survival rates of WT p*fur*, $\Delta ydiU$ p*fur*, WT p*fur*H118A, and $\Delta ydiU$ p*fur*H118A strains after metal deprivation. The above-described experiments were performed as three replicates, and the mean values are presented. ***, $P < 0.001$; **, $P < 0.01$; *, $P < 0.05$; n.s., $P > 0.05$.

contrast, the expression of YdiU slightly decreased the expression of iron uptake genes in the Δfur strain, suggesting that activation of iron uptake by YdiU depended on Fur. Our previous study showed that *ydiV*, the gene next to *ydiU* on the chromosome, modulates iron homeostasis by changing the conformation of Fur with the assistance of SlyD in *Escherichia coli* (27). To test the potential role of YdiV in YdiU-mediated iron regulation in *Salmonella*, we constructed $\Delta ydiV$ and YdiU-expressing $\Delta ydiV$ ($\Delta ydiV$ pydiU) strains and detected the mRNA levels of *entE* and *fepA* (Fig. 5E). The results showed drastically activated expression levels of *entE* and *fepA* by YdiU in both strains, suggesting that regulation of iron uptake by YdiU was independent of YdiV. To further determine the impact of YdiU on Fur-mediated inhibition of iron uptake, we constructed Fur-expressing WT and $\Delta ydiU$ strains, WT p*fur* and $\Delta ydiU$ p*fur*, respectively. We challenged WT p*fur* and $\Delta ydiU$ p*fur* strains with iron deficiency stress and observed significantly decreased survival for $\Delta ydiU$ p*fur* compared with that of WT p*fur* (Fig. 5F). To determine the role of H118-specific UMPylation, WT and $\Delta ydiU$ Fur H118A-overexpressing strains were constructed and treated with iron deficiency stress (Fig. 5F). The survival rate of WT p*fur*H118A displayed a significant reduction compared to WT p*fur*, with no statistical difference observed between WT p*fur*H118A and $\Delta ydiU$ p*fur*H118A. Collectively, these results suggest that activation of iron uptake by YdiU was indeed achieved by blocking the inhibitory effect of Fur on iron uptake through UMPylation of Fur on H118.

YdiU-mediated regulation of iron uptake facilitates *Salmonella* infection. To investigate the function of YdiU during host infection of *Salmonella*, HT-29 cells were infected with WT or $\Delta ydiU$ strains at the same multiplicity of infection (MOI). HT29 cells were lysed 2 h, 4 h, and 6 h postinfection, and then the expression levels of *Salmonella ydiU*, *fur*, and iron uptake genes were detected by qPCR (Fig. 6). Compared with the sample prior to invasion, the expression of *ydiU* increased 13.26-, 14.01-, and 9.85-fold 2, 4, and 6 h after WT *Salmonella* invasion, with no expression of *ydiU* detected in the $\Delta ydiU$ strain (Fig. 6A). The expression of *fur* in the $\Delta ydiU$ strain did not significantly differ from that of the WT strain during infection (Fig. 6B), while the expression of iron uptake genes in $\Delta ydiU$ strain was significantly decreased compared with the WT strain (Fig. 6C to E). Consistent with previous studies (36), the expression of iron uptake genes in WT strain increased 10- to 20-fold when measured 2 h postinvasion (21.03-fold for *entE*, 26.50-fold for *fepA*, and 11.27-fold for *fes*). However, the expression of iron uptake genes did not significantly increase in the $\Delta ydiU$ strain after invasion (1.63-fold for

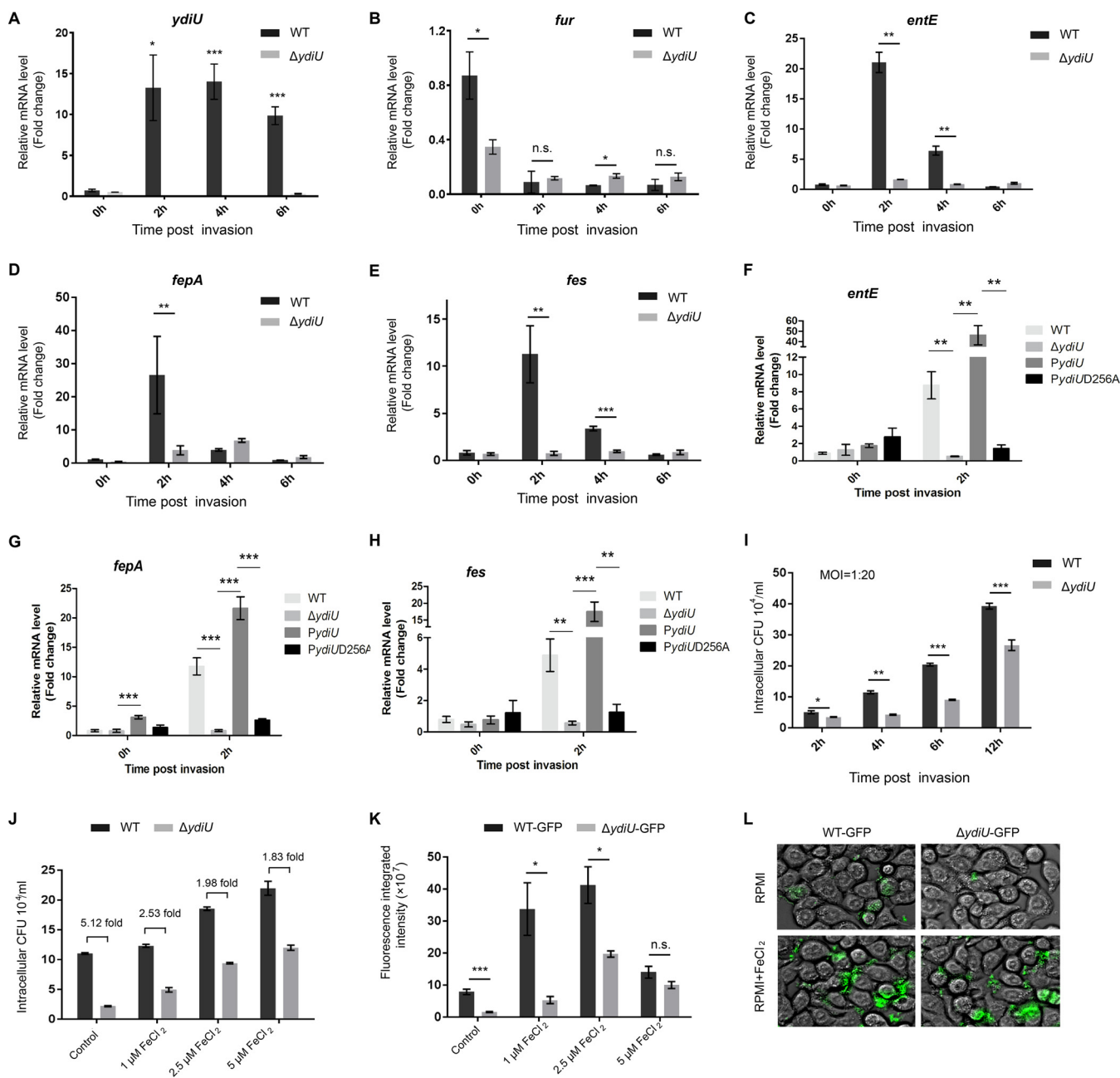


FIG 6 YdiU effectively activates *Salmonella* iron uptake within host cells. (A) *Salmonella* upregulates YdiU expression during invasion. The mRNA levels of *ydiU* before and after *Salmonella* invasion were detected in WT and $\Delta ydiU$ strains by qRT-PCR. (B) YdiU did not inhibit the expression of Fur. The mRNA levels of *fur* before and after *Salmonella* invasion were detected in WT and $\Delta ydiU$ strains by qRT-PCR. (C to E) The mRNA levels of *entE* (C), *fepA* (D), and *fes* (E) before and after *Salmonella* invasion were detected in WT and $\Delta ydiU$ strains by qRT-PCR. The transcription levels of *entE* (F), *fepA* (G), and *fes* (H) before and after WT, $\Delta ydiU$, $\Delta ydiU$ *pydiU*, and $\Delta ydiU$ *pydiUD256A* entering HT29 cells were detected by qRT-PCR. (I) The intracellular amounts of bacteria were quantified in HT-29 cells at the indicated times postinfection. (J) The intracellular amounts of WT and $\Delta ydiU$ strains were quantified in HT-29 cells cultured with different concentrations of FeCl₂. (K) The fluorescence integrated intensity was applied and quantified with GFP-expressing *Salmonella*-infected HT-29 cells cultured in medium with different concentrations of FeCl₂. (L) HT-29 cells infected with GFP-expressing WT and $\Delta ydiU$ strain cultured in the medium with or without FeCl₂. Experiments were performed with at least three replicates, and the mean values are presented. ***, $P < 0.001$; **, $P < 0.01$; *, $P < 0.05$; n.s., $P > 0.05$.

entE, 3.8-fold for *fepA*, and 0.74-fold for *fes*), demonstrating that YdiU is required for efficient activation of iron acquisition during *Salmonella* infection. As further confirmation, we conducted complementation experiments of $\Delta ydiU$ strain with native *ydiU* or the *ydiU* D256A mutant. As expected, the insufficient expression levels of iron uptake genes (*entE*, *fepA*, and *fes*) in $\Delta ydiU$ mutant within host cells can be rescued by native YdiU but not by the YdiU D256A mutant (Fig. 6F to H).

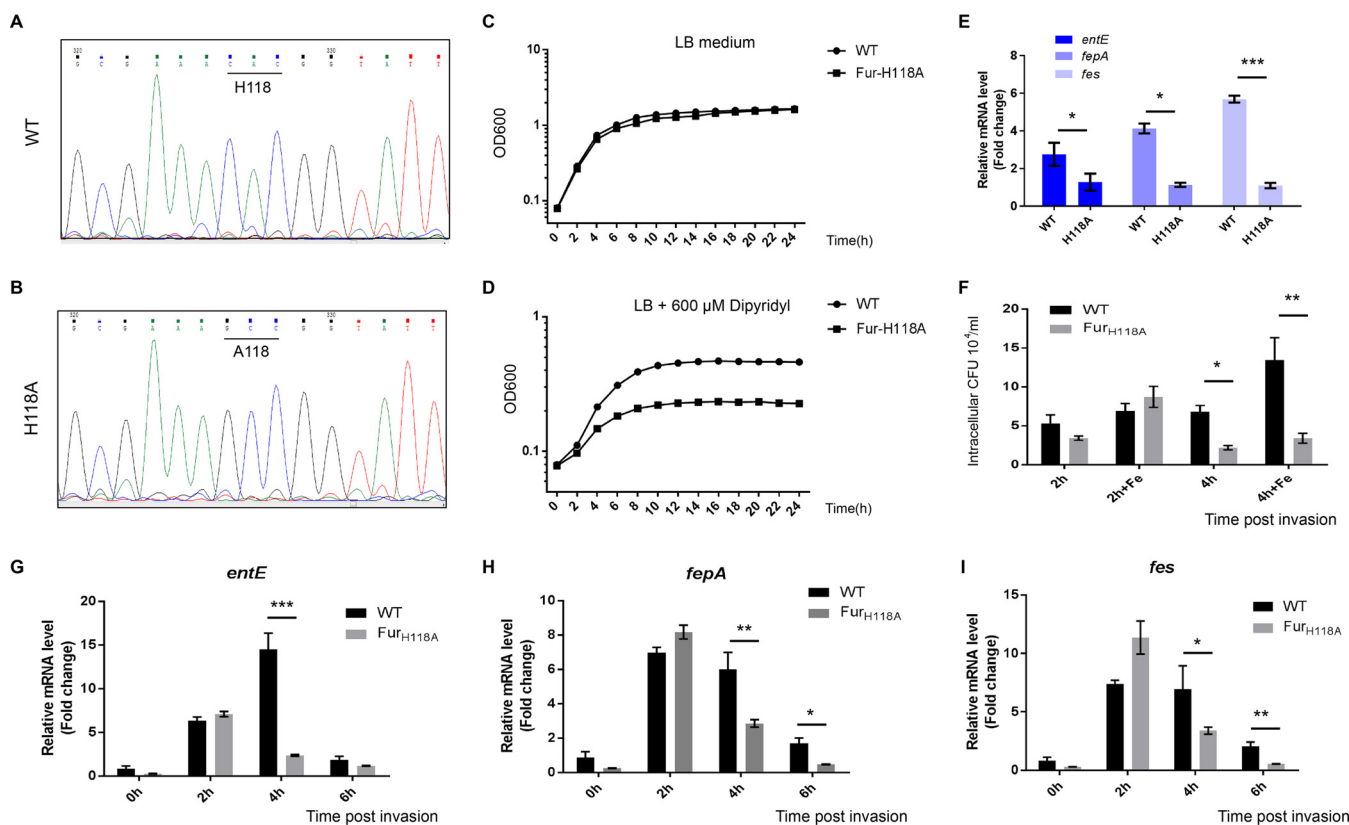


FIG 7 Fur H118 is essential for *Salmonella* survival under iron deficiency conditions and during infection. (A and B) Sanger sequencing results of wild-type strain (A) and Fur H118A (B) mutant strain. (C and D) The growth curves of WT and H118A mutant strains cultivated in LB medium or metal-limited medium. (E) The transcription levels of iron uptake genes (*entE*, *fepA*, and *fes*) in WT and H118A mutant strains cultured under metal deficiency condition. (F) The intracellular amounts of bacteria were quantified in HT-29 cells at the indicated times postinfection. HT-29 cells were cultured in the medium with or without FeCl₂. (G to I) The mRNA levels of *entE* (G), *fepA* (H), and *fes* (I) before and after invasion were detected in WT and H118A mutant strains. Experiments were performed in at least three replicates, and the mean values are presented. ***, $P < 0.001$; **, $P < 0.01$; *, $P < 0.05$; n.s., $P > 0.05$.

Given that acquisition of iron is a prerequisite for *Salmonella* survival in host cells (21, 34), we hypothesize that YdiU facilitates *Salmonella* survival within host cells. To test this hypothesis, we measured the survival of WT and $\Delta ydiU$ strains at various times after entry of *Salmonella* into HT-29 cells. The amounts of intracellular bacteria in host cells were determined by counting CFU 2 h, 4 h, 6 h, and 12 h postinvasion. Compared with the WT strain, the $\Delta ydiU$ strain showed significantly attenuated ability to colonize in HT-29 cells (Fig. 6I). When iron was added to the cell culture, the survival difference between WT and $\Delta ydiU$ strains decreased from 5.12-fold to 1.83-fold, suggesting that the decline in survival of $\Delta ydiU$ strain within host cells was partially caused by the deficiency in iron uptake (Fig. 6J). To further investigate the effect of YdiU on *Salmonella* infection *in vivo*, green fluorescent protein (GFP)-expressing WT (WT-GFP) and GFP-expressing $\Delta ydiU$ ($\Delta ydiU$ -GFP) strains were constructed and used to infect HT-29 cells. FeCl₂ was added to the cell culture to observe the effect of iron on intracellular survival of *Salmonella*. Fluorescence intensity was measured to determine bacterial count. The results clearly showed that the addition of FeCl₂ to cell culture improved survival for both WT-GFP and $\Delta ydiU$ -GFP strains (Fig. 6K and L). Consistent with Fig. 6J, the imaging results also support the effect of iron addition to improve the inhibited growth of $\Delta ydiU$ -GFP strain compared with WT-GFP (Fig. 6L).

H118 of Fur is essential for the activation of iron uptake pathway during *Salmonella* infection. To further investigate the function of Fur UMPylation on iron metabolism, a single nucleotide polymorphism was inserted into wild-type *Salmonella* to generate a Fur H118A mutant strain that cannot be regulated by YdiU-mediated UMPylation, so it would restrict Fur in the deUMPylated state (Fig. 7A and B). Similar to what we observed in the $\Delta ydiU$ strain (Fig. 1F and G), a serious growth defect of Fur H118A was observed under metal-deficient conditions but not in LB medium (Fig. 7C and D). The expression levels of iron uptake

genes in WT and Fur H118A strain under iron deficiency conditions were detected by qPCR (Fig. 7E). Compared with the WT strain, there was dramatically decreased transcription of iron uptake genes in the H118A strain under iron-deficient conditions: 0.36-fold for *entE*, 0.24-fold for *fepA*, and 0.18-fold for *fes*. The numbers of CFU of WT and H118A strains were determined 2 h and 4 h postinvasion into HT-29 cells (Fig. 7F). No significant difference was observed 2 h postinvasion; however, the H118A strain exhibited significantly attenuated survival in HT-29 cells 4 h postinvasion compared with the WT strain (Fig. 7F). Additionally, the expression of iron uptake genes in the H118A strain was markedly reduced compared with the WT strain 4 h postinfection: 0.16-fold for *entE*, 0.48-fold for *fepA*, and 0.50-fold for *fes* (Fig. 7G to I). The above-described data indicate that restricting Fur in the deUMPylated state dramatically eliminates *Salmonella* iron uptake under iron deficiency environments and therefore limits *Salmonella* proliferation within host cells.

DISCUSSION

When bacteria enter host cells, obtaining enough iron from the host is critical for bacterial colonization and intracellular survival (7, 20). The Fur protein is the most critical negative regulator of bacterial iron adsorption (17, 39, 41). Interestingly, when bacteria enter host cells, the expression of Fur remains high, but bacteria can upregulate the expression of iron absorption-related genes 10- to 20-fold to rapidly initiate iron absorption (36, 37). According to the classical model, iron ions regulate Fur binding to promoters of iron absorption genes. When the iron ion concentration is low, Fur protein is released from its target DNA sequences, allowing RNA polymerase to bind and transcribe the iron absorption genes (18). However, there are limitations of this simple iron regulation model. First, both *in vivo* and *in vitro* studies show that Fur can bind to iron, manganese, and nickel ions, and all three allow DNA binding activity (25). Bacteria can absorb large amounts of extracellular manganese ions when they enter an iron-deficient condition, increasing the intracellular manganese ion concentration up to 20-fold (42, 43). Therefore, it may not be possible to completely regulate Fur protein function only by control of iron concentration. YdiU-mediated UMPylation of Fur probably works in this event. YdiU is an obligatory Mn-dependent UMPylator. The intracellular Mn^{2+} concentration of bacteria is actually elevated in an iron-deficient environment, and UMPylation of Fur by YdiU is initiated by Mn^{2+} . Since Fur can bind Mn and Fe ions indistinguishably, Mn can metallate Fur and activate DNA binding by Fur. UMPylation might function as a regulatory switch to effectively prevent Mn-activated iron uptake inhibition of Fur. YdiU may be a key link allowing *Salmonella* to sense the Mn/Fe ratio and turn on the low-Fe regulatory response.

Previous studies have found that the EAL-like protein YdiV can transform Fur into a state that cannot bind to DNA with the help of SlyD (27). YdiV is next to YdiU on the chromosome, and here we found that YdiU can inhibit Fur's DNA binding activity by posttranslational modification, thus rapidly promoting iron absorption. YdiV and YdiU have similar functions, as both proteins turn off flagellar synthesis and initiate iron uptake. Interestingly, YdiV and YdiU exert their functions through completely different mechanisms, YdiV through protein interaction and YdiU through UMPylation, suggesting these two proteins function independently of each other. However, since these two genes are close to each other on the chromosome, they may be regulated by the same transcription factors (nutrient deficiency induces expression of both YdiU and YdiV), and there will likely be some synergy in expression regulation.

Based on the results of this study, we propose the following mechanistic model (Fig. 8). When *Salmonella* grow in an iron-rich environment, the Fur protein binds to the promoter region of the iron absorption gene, inhibiting the recruitment of RNA polymerase and minimizing iron absorption. When *Salmonella* enter host cells, YdiU protein expression is activated by iron deficiency, high reactive oxygen species, and low pH. YdiU uses UTP to transfer a UMP group to H118 of Fur, preventing Fur dimerization. Fur is displaced from the promoter region of iron absorption genes, thus allowing its activation. Through this mechanism, *Salmonella* obtain enough iron to survive inside host cells. The identified modification sites are highly conserved in homologous proteins (see Fig. S6 in the supplemental material), suggesting that this Fur regulatory mechanism is widespread. The covalent attachment mode of UMP to histidine is similar to that of phosphorylated histidine

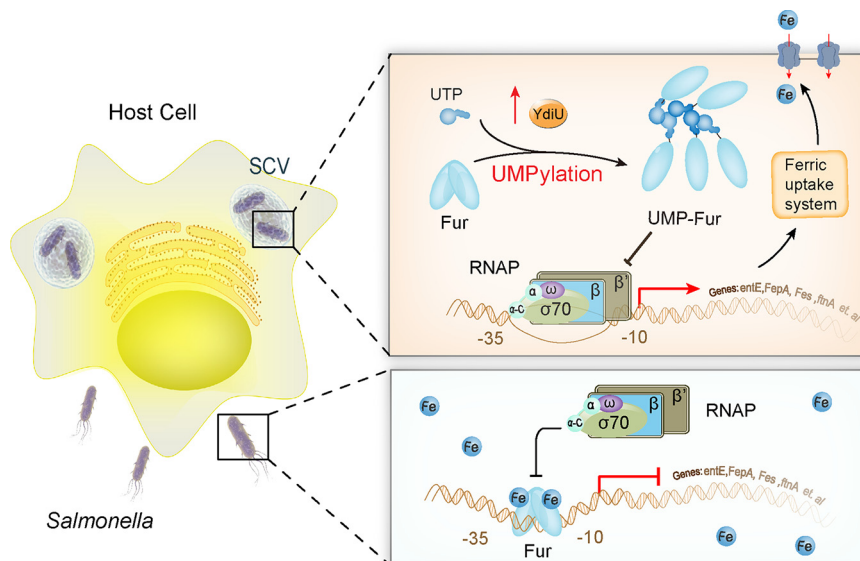


FIG 8 Model of YdiU-mediated iron uptake regulation during *Salmonella* infection. Before *Salmonella* enters host cells, iron-bound Fur can inhibit the transcription of iron uptake genes. When *Salmonella* enters host cells and is subjected to iron-deficient conditions, the expression of YdiU is induced by stress signaling. YdiU then modifies Fur with UMP on its H118 residue. UMPylated Fur is removed from the promoters of iron uptake genes, relieving the inhibition of the iron uptake genes by Fur. Bacteria will take up more iron through iron carriers, increasing survival in host cells.

(pHis), which plays a crucial role in prokaryotic signal transduction (44, 45). Because pHis is a labile posttranslational modification under acid conditions, a similar acid lability of UMP-His was assumed. Furthermore, we speculate that a de-UMPylase, analogous to pHis phosphatases (46), regulates UMPylated proteins dynamically.

Quantitative proteomic analysis demonstrated YdiU regulated cell motility, iron homeostasis, virulence, and energy production in *Salmonella* under iron deficiency conditions (Fig. S1). Previous studies showed that Fur is not only a key regulator of iron absorption but also indirectly affects expression of 20% of bacterial proteins and is involved in pathogenicity, acid tolerance, and nitrate respiration of *Salmonella* (47–49). Thus, it is possible that regulatory activities of YdiU in addition to iron homeostasis are controlled by the UMPylation of Fur. To our knowledge, UMPylation is the first posttranslational modification found to regulate Fur function. Fur was found to be UMPylated at H33 in our previous study, and H118 was not identified as a site of UMPylation in those data (28). The UMPylated peptides in our 2020 study were identified from proteomics data using whole bacterial proteins, and this may explain the lack of detection of Fur H118 UMPylation. In this study, UMPylation of Fur H118 was observed both *in vitro* and *in vivo*, and more importantly, the single mutation of H118 led to a significant decrease in bacterial survival under iron-deficient conditions, demonstrating H118 is a critical site for Fur activity. According to these observations, we propose that posttranslational modification plays a crucial role in the regulation of Fur.

MATERIALS AND METHODS

Bacterial strains and culture conditions. All bacterial strains are listed in Table S1 in the supplemental material. Generally, strains were propagated in Luria-Bertani medium at 37°C with shaking at 200 rpm, and LB agar plates contained 1.5% (wt/vol) agar supplemented with antibiotics and 2,2'-dipyridyl as required. For iron stress experiments, the strains were activated in LB medium overnight, and then cultures were transferred to fresh medium at an OD_{600} of 0.01 for homogenized growth. When strains entered mid-log phase ($OD_{600} = 0.6$), 2,2'-dipyridyl was added at the indicated concentrations. For the experiments shown in Fig. 1A and B and 2E, log-phase *Salmonella* cultures were treated with different concentrations of 2,2'-dipyridyl (200 to 600 μ M) for 6 h. For the experiments shown in Fig. 1C and D and 2F, when strains entered mid-log phase, 600 μ M 2,2'-dipyridyl was added to induce gene expression, and samples with no 2,2'-dipyridyl were used as a control (0 h). The cultures were sampled at 1 h, 2 h, or 3 h. For the experiments shown in Fig. S2 and S3C and Fig. 5A to E and 7E, log-phase *Salmonella* cultures were treated with 600 μ M 2,2'-dipyridyl for 3 h.

RNA extraction and qRT-PCR. Total RNA was isolated using SPARKeasy Bacteria RNA kit (Sparkjade) or RNAPrep Pure Cell/Bacteria kit (Tiangen). Reverse transcription reactions were performed using the

RevertAid cDNA synthesis kit (Thermo) according to the manufacturer's instructions. Quantitative real-time-PCR (qRT-PCR) reactions were performed on an Applied Biosystems 7500 sequence detection system (Applied Biosystems) using iTaq Universal SYBR green supermix (Bio-Rad).

Western blotting. Bacterial cells were lysed using 1 × loading buffer and then heated at 95°C for 10 min before SDS-PAGE. Total proteins were examined by 12% SDS-PAGE and then electrotransferred onto a polyvinylidene fluoride (PVDF) membrane (Millipore). The membranes were blocked with 5% milk in phosphate-buffered saline plus Tween (PBST) at 25°C for 1 h, followed by incubation overnight at 4°C with polyclonal antibody to YdiU (1:2,000 dilution) or GapA (1:10,000 dilution) in PBST. After three washes with PBST, the membranes were then incubated at 25°C for 1 h with horseradish peroxidase (HRP)-conjugated goat anti-rabbit or mouse IgG (Abcam) diluted 1:10,000 in PBST. Finally, the membranes were incubated with a chemiluminescent substrate (Immobilon Western HRP substrate; Millipore) and detected using a FluorChem imager (Uvitec).

Survival rate under metal deficiency condition. Wild-type and $\Delta ydiU$ strains were grown to logarithmic phase in LB medium, and then 2,2'-dipyridyl was added to the bacterial solution to a final concentration of 800 μM . Samples were removed after exposure to 2,2'-dipyridyl for 3 h and then serially diluted into PBS (pH 7.4). For the experiments shown in Fig. 1E and 5F, 250- μL samples of 10^6 bacteria were plated on LB agar plates. Plates were incubated at 37°C for 24 h and the colonies were counted. The percentage of bacterial survival was determined (with time zero representing 100%) as a function of the duration of iron deficiency.

Growth under metal-deficient condition. For the experiments shown in Fig. 1F and G and 7C and D, bacterial growth was measured using a Bioscreen C automatic growth analyzer at 37°C with a honeycomb microplate. To measure growth, bacteria were diluted into LB medium plus 400 μM 2,2'-dipyridyl, 300 μL of diluted culture were added into individual wells, and each strain was assayed in triplicate. Samples were measured at 600-nm absorbance every 5 min for 24 h. For the iron-add-back experiments shown in Fig. 1H, WT and $\Delta ydiU$ *Salmonella* cells were cultured in LB medium plus 600 μM 2,2'-dipyridyl. Two hours after the start of culturing, different concentrations of FeCl_2 were added back to the medium, and the OD₆₀₀ values were monitored in real time.

Sample preparation for mass spectrometry-based proteomic analysis. Wild-type and $\Delta ydiU$ strains were grown to logarithmic phase in LB medium, and then 2,2'-dipyridyl was added to the bacterial solution to a final concentration of 600 μM and allowed to culture at 37°C for 3 h. The bacteria were then pelleted by centrifugation and lysed using a buffer containing 8 M urea, 1% Triton X-100, 10 mM dithiothreitol, and 2 mM EDTA. After centrifugation of the samples at 20,000 × *g* for 10 min, the supernatants were removed and the amount of protein quantified with the bicinchoninic acid (BCA) protein assay kit (Beyotime). Samples of 200 μg protein were purified by ultrafiltration, incubated with iodoacetamide to block reduced cysteine residues, and then digested with 4 μg trypsin at 37°C overnight. Peptides of each sample were desalted on C₁₈ cartridges, concentrated by vacuum centrifugation, and reconstituted in 40 μL of 0.1% (vol/vol) formic acid.

TMT quantitative proteomic analysis. Tandem mass tag (TMT) quantitative proteomic analysis was performed by Jingjie Biological Technology Co., Ltd. (Hangzhou, China). In brief, total protein was extracted from wild-type and $\Delta ydiU$ cells using a high-intensity ultrasonic processor (Scientz) in lysis buffer (8 M urea, 1% protease inhibitor cocktail; Roche). The cell lysates were collected and quantified with the BCA protein assay kit (Beyotime) according to the manufacturer's instructions. For trypsin digestion, the protein solution was reduced with 5 mM dithiothreitol and then alkylated with 11 mM iodoacetamide according to a previous study (50). The digested samples then were desalted by a Strata X-C18-SPE column (Phenomenex, Torrance, CA, USA) and vacuum dried. For TMT labeling, we reconstituted peptides in 0.5 M TEAB (TMT kit; Thermo Scientific, Waltham, MA, USA) and processed them according to the manufacturer's protocol. For sample preparation, the tryptic peptides were fractionated by high-pH (using a gradient of 8% to 32% acetonitrile, pH 9.0), reverse-phase high-performance liquid chromatography (HPLC) using an Agilent 300Extend C₁₈ column (5- μm particles, 4.6-mm inner diameter, 250-mm length). Running of samples in liquid chromatography-tandem mass spectrometry (LC-MS/MS) and analysis were performed as described before (51).

ICP-MS. *Salmonella* strains were inoculated into iron-rich LB medium or iron-limited LB medium (final concentration of 600 μM 2,2'-dipyridyl was added) and cultured to an OD₆₀₀ of 1.0. Cells were collected and washed twice using PBS solution supplemented with 5 mM EDTA to remove ions from the medium and then washed twice using PBS (without EDTA) to remove EDTA. Finally, the cells were dried at 60°C overnight. Next, 0.2-g samples were weighed and transferred to a Teflon digestion tank together with 5 mL nitric acid. After the reaction was complete, the cover was sealed and put into a microwave digestion instrument. After the temperature cooled to below 50°C, the digestion tank was removed, moved to a fume hood, and opened. The sample was resuspended in ultrapure water and transferred to a 50-mL volumetric flask, with three to four cycles of moistening and washing. Samples were then diluted in 20 mL of deionized water and filtered for final analysis using inductively coupled plasma mass spectrometry (ICP-MS) (Thermo iCAPQ). Three biological replicates were performed per sample.

Generation of constructs and strains. All plasmids used in this study are listed in Table S2. *Salmonella* Fur and FurH118A genes were cloned into the pBAD24 vector for *in vivo* study. For biochemical study, *ydiU* and *fur* genes were amplified from *E. coli* K-12 substrain MG1655 genomic DNA and cloned into the pGL01 vector, which is a modified expression vector based on pET15b with a PPase cleavage site to remove the His tag. Mutants of FurH118A were constructed using the Mut Express II fast mutagenesis kit V2 (Vazyme, Nanjing) and separately cloned into pBAD24 and pGL01.

The gene knockout mutant of Fur was constructed using the lambda Red recombinase system as described previously (52). YdiU D248A mutant strain and Fur H118A mutant strain were constructed by CRISPR/Case9 with the help of Guangzhou Ubigen Biosciences Co., Ltd.

Protein expression and purification. Both YdiU and Fur used for purification were from *E. coli*. Proteins were expressed in *E. coli* BL21(DE3) or *E. coli* BL21(DE3) *ydiU* knockout strain. Expression and purification

of *E. coli* YdiU were performed as described previously (53). To obtain Fur without UMPylation, the *E. coli* BL21 (DE3) *ydiU* knockout strain was used. Briefly, when the OD₆₀₀ reached 0.6, cultures were cooled to 16°C and protein expression was induced overnight by 0.1 mM isopropyl-β-D-thiogalactopyranoside (IPTG). Harvested cells were lysed by sonication, and proteins were purified by Ni²⁺-nitrilotriacetic acid (NTA) affinity column. The His tag of the proteins was removed by PPase treatment (54), and then proteins were concentrated and purified by Superdex 200 chromatography. To obtain Fur with UMPylation, Fur and YdiU were coexpressed in *E. coli* BL21 (DE3) and purified as described above.

In vitro UMPylation assay with biotin-UTP. *In vitro* UMPylation assays were performed as described previously (28). Briefly, 4 μg of purified *E. coli* Fur or FurH118A was incubated with or without 1 μg *E. coli* YdiU⁴⁷⁵ in a 20-μL reaction buffer containing 25 mM Tris-HCl (pH 7.5), 100 mM NaCl, 10 mM MnCl₂, and 200 μM biotin-16-UTP at 30°C for 1 h. The Streptavidin HRP blot then was performed as previously described (28).

Identification of UMPylation sites by MS. UMPylated proteins were analyzed on 12% NuPAGE gel and stained with Coomassie brilliant blue. The protein bands of *E. coli* Fur were excised from the gel and digested overnight with trypsin. The digested peptides were desalted using a ZipTip C₁₈ column (Millipore, Billerica, MA) for the subsequent LC-MS/MS analysis. About 2 μg of the trypsin-digested peptides was injected into a C₁₈ column and eluted with a linear gradient from 5% acetonitrile to 35% acetonitrile, followed by using the Orbitrap Elite mass spectrometer (Thermo Fisher). Data were acquired for the 20 most intense peaks of every full MS scan. MS/MS spectra were searched against the *Escherichia coli* (strain K-12) database (UniProt no. 83333) using Mascot. MS/MS spectra were searched with a maximum mass tolerance of 10 ppm for the precursors, 0.6 Da for fragments, dynamic UMPylation (306.025302, H₁C₃N₂O₈P) for Tyr, His, Ser, Thr, and methionine oxidation, and missed cleavage of 2.

Size-exclusion chromatography. For the size-exclusion chromatography experiment presented in Fig. 3F, 100 μg *E. coli* Fur^{dYdiU} and/or 100 μg *E. coli* Fur^{pYdiU} proteins was analyzed by size-exclusion chromatography using a Superdex 200 column. A 53-kDa protein and a 22-kDa protein were examined by size-exclusion chromatography under the same conditions as controls.

DLS. Dynamic light scattering (DLS) was applied to determine the hydrodynamic radius (rH) of protein samples. Measurements were performed in a 96-well plate at 25.0 ± 0.1°C using a DynaPro plate reader 3 (Wyatt Technology, Santa Barbara, California). Proteins were diluted to 0.5 mg/mL, with 100 μL sample per well. Data processing was automatically performed by the software supplied with the instrument.

Native PAGE. Proteins were obtained as described above. Native PAGE experiments were carried out by 12% acrylamide gel in native PAGE buffer (pH 8.0; Beyotime Biotechnology) at 120V for 1 h. Modified and unmodified Fur proteins were electrophoretically separated, and the gels were scanned by a calibrated densitometer (GS-900; Bio-Rad) after staining with Coomassie brilliant blue.

EMSA. To obtain fluorophore 6-carboxy-fluorescein (FAM)-labeled double-stranded Fur box DNA (GATAATGATAATGATAATGATAATGATAATGA), two reverse complementary single-stranded FAM-Fur box DNA oligonucleotides were mixed to 10 mM in annealing buffer (10 mM Tris-HCl, pH 7.5, 150 mM NaCl), heated at 95°C for 10 min, and slowly cooled to room temperature. Next, 20 nM the annealed DNA was preincubated with different ratios of protein samples at 37°C for 10 min. Samples were resolved on 6% native polyacrylamide gel and electrophoresed in TBE buffer (46 mM Tris base, 46 mM boric acid, 1 mM EDTA, pH 8.0) at 4°C for 60 min at 100 V. Light was avoided in this experiment. Imaging was performed using ChemiDoc MP imaging system (Bio-Rad). Finally, the gel was stained with Coomassie brilliant blue.

Cell culture and bacterial infection experiments. The human colon adenocarcinoma cell line HT-29 was maintained at 37°C with 5% CO₂ in RPMI 1640 medium (Gibco) containing 10% fetal bovine serum (Gibco). Cells were seeded at 1 × 10⁷ in 100-mm tissue culture dishes. Bacteria were cultured in LB medium to OD₆₀₀ of 0.5, diluted into RPMI 1640 medium, and then seeded on HT-29 cells at a multiplicity of infection (MOI) of 20. After 1 h of infection, the bacteria were removed from plates. The cells were washed twice with PBS, and then RPMI 1640 with gentamicin (100 μg/mL) was added to kill the remaining extracellular bacteria. The cells were washed twice, and RPMI 1640 with gentamicin (20 μg/mL) was added to keep the cells alive and inhibit extracellular bacteria. At different time points after infection (2 h, 4 h, or 6 h), cells were washed and lysed in TRIzol reagent (Tiangen) and then stored at -80°C for RNA extraction. Bacteria before invasion were used for the control (0 h). For the experiments shown in Fig. S8, four strains, WT, *ΔydiU*, *ΔydiU pydiU*, and *ΔydiU pydiUD256A* strains, were cultured in LB medium to OD₆₀₀ of 0.2 before addition of L-arabinose to a final concentration of 0.5% to induce YdiU/YdiUD256A expression. After 1 h, cell invasion experiments were performed as described above. For the experiments shown in Fig. 6I and 7F, after infection, cells were washed gently and disrupted with 1% Triton X-100 (Sigma Chemical) at different time points, and then serial dilutions of bacteria were plated on LB agar to determine the number of CFU. For the experiments shown in Fig. 6J, various concentrations of FeCl₂ (1 μM, 2.5 μM, or 5 μM) were added to RPMI 1640. HT-29 cells cultured without addition of FeCl₂ were used as a control.

Fluorescence microscopy. HT-29 cells were cultured in 96-well format with various concentrations of FeCl₂. WT and *ΔydiU Salmonella* expressing GFP were cultured in LB medium to an OD₆₀₀ of 0.5, diluted using RPMI 1640 medium, and seeded on HT-29 cells at an MOI of 20 using previous methods. Fluorescence images were obtained using the Molecular Devices ImageXpress Microconfocal 4 h after infection. After high-throughput image acquisition of the 96-well screening plates (60×; 1 × 10⁵ cells per well), automated image analysis for fluorescence intensity was applied by MetaXpress Imaging and Analysis software.

Statistical analysis. All experiments were performed with three biological replicates unless otherwise stated. A two-tailed Student's *t* test was used to calculate *P* values using GraphPad Prism or SPSS. Error bars represent the standard errors of the means (SEM). The statistical significance is indicated by *P* values of <0.001 (***), <0.01 (**), or <0.05 (*). Statistical details of experiments are included in the figure legends.

Data availability. Proteomic data have been submitted to ProteomeXchange via the PRIDE database (<http://www.ebi.ac.uk/pride>) under the data set identifier PXD023378.

SUPPLEMENTAL MATERIAL

Supplemental material is available online only.

FIG S1, TIF file, 1.8 MB.

FIG S2, TIF file, 0.9 MB.

FIG S3, TIF file, 1.2 MB.

FIG S4, TIF file, 2 MB.

FIG S5, TIF file, 1.9 MB.

FIG S6, TIF file, 1.3 MB.

FIG S7, TIF file, 2 MB.

TABLE S1, DOCX file, 0.02 MB.

TABLE S2, DOCX file, 0.02 MB.

ACKNOWLEDGMENTS

National Natural Science Foundation of China [31900124 to H.H.J, 32000095 to N.N.S., 32170034 to B.Q.L], the Academic Promotion Program of Shandong First Medical University [2019LJ001 to B.Q.L], the Primary Research and Development Plan of Shandong Province (2019GSF107026 to B.Q.L. and 2019GSF107055 to N.N.S.), the Innovation Project of Shandong Academy of Medical Sciences (B.Q.L). Youth Innovation Talent Development Plan of Shandong Provincial University (B.Q.L).

We have no conflict of interest to declare.

REFERENCES

- Hoffbrand AV, Ganeshaguru K, Hooton JW, Tattersall MH. 1976. Effect of iron deficiency and desferrioxamine on DNA synthesis in human cells. *Br J Haematol* 33:517–526. <https://doi.org/10.1111/j.1365-2141.1976.tb03570.x>.
- Kupper H, Setlik I, Seibert S, Prasil O, Setlikova E, Strittmatter M, Levitan O, Lohscheider J, Adamska I, Berman-Frank I. 2008. Iron limitation in the marine cyanobacterium *Trichodesmium* reveals new insights into regulation of photosynthesis and nitrogen fixation. *New Phytol* 179:784–798. <https://doi.org/10.1111/j.1469-8137.2008.02497.x>.
- Cassat JE, Skaar EP. 2013. Iron in infection and immunity. *Cell Host Microbe* 13:509–519. <https://doi.org/10.1016/j.chom.2013.04.010>.
- Neilands JB. 1981. Iron absorption and transport in microorganisms. *Annu Rev Nutr* 1:27–46. <https://doi.org/10.1146/annurev.nu.01.070181.000331>.
- Hood MI, Skaar EP. 2012. Nutritional immunity: transition metals at the pathogen-host interface. *Nat Rev Microbiol* 10:525–537. <https://doi.org/10.1038/nrmicro2836>.
- Weinberg ED. 1975. Nutritional immunity. Host's attempt to withhold iron from microbial invaders. *JAMA* 231:39–41. <https://doi.org/10.1001/jama.1975.03240130021018>.
- Wooldridge KG, Williams PH. 1993. Iron uptake mechanisms of pathogenic bacteria. *FEMS Microbiol Rev* 12:325–348. <https://doi.org/10.1111/j.1574-6976.1993.tb00026.x>.
- Li B, Li N, Yue Y, Liu X, Huang Y, Gu L, Xu S. 2016. An unusual crystal structure of ferric-enterobactin bound FepB suggests novel functions of FepB in microbial iron uptake. *Biochem Biophys Res Commun* 478:1049–1053. <https://doi.org/10.1016/j.bbrc.2016.08.036>.
- Pollack JR, Neilands JB. 1970. Enterobactin, an iron transport compound from *Salmonella typhimurium*. *Biochem Biophys Res Commun* 38:989–992. [https://doi.org/10.1016/0006-291x\(70\)90819-3](https://doi.org/10.1016/0006-291x(70)90819-3).
- Raymond KN, Dertz EA, Kim SS. 2003. Enterobactin: an archetype for microbial iron transport. *Proc Natl Acad Sci U S A* 100:3584–3588. <https://doi.org/10.1073/pnas.0630018100>.
- Qi B, Han M. 2018. Microbial siderophore enterobactin promotes mitochondrial iron uptake and development of the host via interaction with ATP synthase. *Cell* 175:571–582. <https://doi.org/10.1016/j.cell.2018.07.032>.
- Gehring AM, Bradley KA, Walsh CT. 1997. Enterobactin biosynthesis in *Escherichia coli*: isochorismate lyase (EntB) is a bifunctional enzyme that is phosphopantetheinylated by EntD and then acylated by EntE using ATP and 2,3-dihydroxybenzoate. *Biochemistry* 36:8495–8503. <https://doi.org/10.1021/bi970453p>.
- Ozenberger BA, Nahlik MS, McIntosh MA. 1987. Genetic organization of multiple fep genes encoding ferric enterobactin transport functions in *Escherichia coli*. *J Bacteriol* 169:3638–3646. <https://doi.org/10.1128/jb.169.8.3638-3646.1987>.
- Winterbourn CC. 1995. Toxicity of iron and hydrogen peroxide: the Fenton reaction. *Toxicol Lett* 82–83:969–974. [https://doi.org/10.1016/0378-4274\(95\)03532-X](https://doi.org/10.1016/0378-4274(95)03532-X).
- Stojiljkovic I, Hantke K. 1995. Functional domains of the *Escherichia coli* ferric uptake regulator protein (Fur). *Mol Gen Genet* 247:199–205. <https://doi.org/10.1007/BF00705650>.
- Troxell B, Hassan HM. 2013. Transcriptional regulation by ferric uptake regulator (Fur) in pathogenic bacteria. *Front Cell Infect Microbiol* 3:59. <https://doi.org/10.3389/fcimb.2013.00059>.
- van Vliet AH, Stoof J, Vlasblom R, Wainwright SA, Hughes NJ, Kelly DJ, Bereswill S, Bijlsma JJ, Hoogenboezem T, Vandenbroucke-Grauls CM, Kist M, Kuipers EJ, Kusters JG. 2002. The role of the ferric uptake regulator (Fur) in regulation of *Helicobacter pylori* iron uptake. *Helicobacter* 7:237–244. <https://doi.org/10.1046/j.1523-5378.2002.00088.x>.
- Lee JW, Helmann JD. 2007. Functional specialization within the Fur family of metalloregulators. *Biometals* 20:485–499. <https://doi.org/10.1007/s10534-006-9070-7>.
- Deng Z, Wang Q, Liu Z, Zhang M, Machado AC, Chiu TP, Feng C, Zhang Q, Yu L, Qi L, Zheng J, Wang X, Huo X, Qi X, Li X, Wu W, Rohs R, Li Y, Chen Z. 2015. Mechanistic insights into metal ion activation and operator recognition by the ferric uptake regulator. *Nat Commun* 6:7642. <https://doi.org/10.1038/ncomms8642>.
- Collins HL. 2003. The role of iron in infections with intracellular bacteria. *Immunol Lett* 85:193–195. [https://doi.org/10.1016/s0165-2478\(02\)00229-8](https://doi.org/10.1016/s0165-2478(02)00229-8).
- Pan X, Tamilselvan B, Hansen EJ, Daefler S. 2010. Modulation of iron homeostasis in macrophages by bacterial intracellular pathogens. *BMC Microbiol* 10:64. <https://doi.org/10.1186/1471-2180-10-64>.
- Frawley ER, Crouch ML, Bingham-Ramos LK, Robbins HF, Wang W, Wright GD, Fang FC. 2013. Iron and citrate export by a major facilitator superfamily pump regulates metabolism and stress resistance in *Salmonella Typhimurium*. *Proc Natl Acad Sci U S A* 110:12054–12059. <https://doi.org/10.1073/pnas.1218274110>.
- Butcher J, Sarvan S, Brunzelle JS, Couture JF, Stintzi A. 2012. Structure and regulon of *Campylobacter jejuni* ferric uptake regulator Fur define apo-Fur regulation. *Proc Natl Acad Sci U S A* 109:10047–10052. <https://doi.org/10.1073/pnas.1118321109>.
- Friedman YE, O'Brian MR. 2004. The ferric uptake regulator (Fur) protein from *Bradyrhizobium japonicum* is an iron-responsive transcriptional repressor in vitro. *J Biol Chem* 279:32100–32105. <https://doi.org/10.1074/jbc.M404924200>.
- Hamed MY, Neilands JB, Huynh V. 1993. Binding of the ferric uptake regulation repressor protein (Fur) to Mn(II), Fe(II), Co(II), and Cu(II) ions as co-repressors: electronic absorption, equilibrium, and 57Fe Mossbauer studies. *J Inorg Biochem* 50:193–210. [https://doi.org/10.1016/0162-0134\(93\)80025-5](https://doi.org/10.1016/0162-0134(93)80025-5).

26. Choi J, Ryu S. 2019. Regulation of iron uptake by fine-tuning the iron responsiveness of the iron sensor Fur. *Appl Environ Microbiol* 85:e03026-18. <https://doi.org/10.1128/AEM.03026-18>.
27. Zhang F, Li B, Dong H, Chen M, Yao S, Li J, Zhang H, Liu X, Wang H, Song N, Zhang K, Du N, Xu S, Gu L. 2020. YdiV regulates *Escherichia coli* ferric uptake by manipulating the DNA-binding ability of Fur in a SlyD-dependent manner. *Nucleic Acids Res* 48:9571–9588. <https://doi.org/10.1093/nar/gkaa696>.
28. Yang Y, Yue Y, Song N, Li C, Yuan Z, Wang Y, Ma Y, Li H, Zhang F, Wang W, Jia H, Li P, Li X, Wang Q, Ding Z, Dong H, Gu L, Li B. 2020. The YdiU domain modulates bacterial stress signaling through Mn(2+)-dependent UMPylation. *Cell Rep* 32:108161. <https://doi.org/10.1016/j.celrep.2020.108161>.
29. Giel JL, Rodionov D, Liu M, Blattner FR, Kiley PJ. 2006. IscR-dependent gene expression links iron-sulphur cluster assembly to the control of O₂-regulated genes in *Escherichia coli*. *Mol Microbiol* 60:1058–1075. <https://doi.org/10.1111/j.1365-2958.2006.05160.x>.
30. Nesbit AD, Giel JL, Rose JC, Kiley PJ. 2009. Sequence-specific binding to a subset of IscR-regulated promoters does not require IscR Fe-S cluster ligation. *J Mol Biol* 387:28–41. <https://doi.org/10.1016/j.jmb.2009.01.055>.
31. Yang J, Tan G, Zhang T, White RH, Lu J, Ding H. 2015. Deletion of the proposed iron chaperones IscA/SufA results in accumulation of a red intermediate cysteine desulfurase IscS in *Escherichia coli*. *J Biol Chem* 290:14226–14234. <https://doi.org/10.1074/jbc.M115.654269>.
32. Dudkiewicz M, Szczepińska T, Grynberg M, Pawłowski K. 2012. A novel protein kinase-like domain in a selenoprotein, widespread in the tree of life. *PLoS One* 7:e32138. <https://doi.org/10.1371/journal.pone.0032138>.
33. Nagy TA, Moreland SM, Andrews-Polymenis H, Detweiler CS. 2013. The ferric enterobactin transporter Fep is required for persistent *Salmonella enterica* serovar typhimurium infection. *Infect Immun* 81:4063–4070. <https://doi.org/10.1128/IAI.00412-13>.
34. Pollack JR, Ames BN, Neilands JB. 1970. Iron transport in *Salmonella typhimurium*: mutants blocked in the biosynthesis of enterobactin. *J Bacteriol* 104:635–639. <https://doi.org/10.1128/jb.104.2.635-639.1970>.
35. Tsolis RM, Baumler AJ, Stojiljkovic I, Heffron F. 1995. Fur regulon of *Salmonella typhimurium*: identification of new iron-regulated genes. *J Bacteriol* 177:4628–4637. <https://doi.org/10.1128/jb.177.16.4628-4637.1995>.
36. Srikumar S, Kroger C, Hebrard M, Colgan A, Owen SV, Sivasankaran SK, Cameron AD, Hokamp K, Hinton JC. 2015. RNA-seq brings new insights to the intra-macrophage transcriptome of *Salmonella Typhimurium*. *PLoS Pathog* 11:e1005262. <https://doi.org/10.1371/journal.ppat.1005262>.
37. Liu Y, Yu K, Zhou F, Ding T, Yang Y, Hu M, Liu X. 2017. Quantitative proteomics charts the landscape of *Salmonella* carbon metabolism within host epithelial cells. *J Proteome Res* 16:788–797. <https://doi.org/10.1021/acs.jproteome.6b00793>.
38. Sreelatha A, Yee SS, Lopez VA, Park BC, Kinch LN, Pilch S, Servage KA, Zhang J, Jiou J, Karasiewicz-Urbańska M, Łobočka M, Grishin NV, Orth K, Kucharczyk R, Pawłowski K, Tomchick DR, Tagliabracchi VS. 2018. Protein AMPylation by an evolutionarily conserved pseudokinase. *Cell* 175:809–821. <https://doi.org/10.1016/j.cell.2018.08.046>.
39. Escolar L, Perez-Martin J, de Lorenzo V. 1999. Opening the iron box: transcriptional metalloregulation by the Fur protein. *J Bacteriol* 181:6223–6229. <https://doi.org/10.1128/JB.181.20.6223-6229.1999>.
40. Agriesti F, Roncarati D, Musiani F, Del Campo C, Iurlaro M, Sparla F, Ciurli S, Danielli A, Scarlato V. 2014. FeON-FeOFF: the *Helicobacter pylori* Fur regulator commutates iron-responsive transcription by discriminative readout of opposed DNA grooves. *Nucleic Acids Res* 42:3138–3151. <https://doi.org/10.1093/nar/gkt1258>.
41. Parro V, Moreno-Paz M. 2004. Nitrogen fixation in acidophile iron-oxidizing bacteria: the nif regulon of *Leptospirillum ferrooxidans*. *Res Microbiol* 155:703–709. <https://doi.org/10.1016/j.resmic.2004.05.010>.
42. Boyer E, Bergevin I, Malo D, Gros P, Cellier MF. 2002. Acquisition of Mn(II) in addition to Fe(II) is required for full virulence of *Salmonella enterica* serovar Typhimurium. *Infect Immun* 70:6032–6042. <https://doi.org/10.1128/IAI.70.11.6032-6042.2002>.
43. Kehres DG, Janakiraman A, Schlauch JM, Maguire ME. 2002. SitABCD is the alkaline Mn(2+) transporter of *Salmonella enterica* serovar Typhimurium. *J Bacteriol* 184:3159–3166. <https://doi.org/10.1128/JB.184.12.3159-3166.2002>.
44. Puttick J, Baker EN, Delbaere LT. 2008. Histidine phosphorylation in biological systems. *Biochim Biophys Acta* 1784:100–105. <https://doi.org/10.1016/j.bbapap.2007.07.008>.
45. Pirrung MC. 1999. Histidine kinases and two-component signal transduction systems. *Chem Biol* 6:R167–R175. [https://doi.org/10.1016/S1074-5521\(99\)80044-1](https://doi.org/10.1016/S1074-5521(99)80044-1).
46. Klumpp S, Krieglstein J. 2002. Phosphorylation and dephosphorylation of histidine residues in proteins. *Eur J Biochem* 269:1067–1071. <https://doi.org/10.1046/j.1432-1033.2002.02755.x>.
47. Ellermeier JR, Schlauch JM. 2008. Fur regulates expression of the *Salmonella* pathogenicity island 1 type III secretion system through HiiD. *J Bacteriol* 190:476–486. <https://doi.org/10.1128/JB.00926-07>.
48. Hall HK, Foster JW. 1996. The role of fur in the acid tolerance response of *Salmonella typhimurium* is physiologically and genetically separable from its role in iron acquisition. *J Bacteriol* 178:5683–5691. <https://doi.org/10.1128/jb.178.19.5683-5691.1996>.
49. Teixeira L, Cortes P, Bigas A, Alvarez G, Barbe J, Campoy S. 2010. Control by Fur of the nitrate respiration regulators NarP and NarL in *Salmonella enterica*. *Int Microbiol* 13:33–39. <https://doi.org/10.2436/20.1501.01.108>.
50. Yun T, Hua J, Ye W, Yu B, Chen L, Ni Z, Zhang C. 2018. Comparative proteomic analysis revealed complex responses to classical/novel duck reovirus infections in *Cairna moschata*. *Sci Rep* 8:10079. <https://doi.org/10.1038/s41598-018-28499-3>.
51. Lin Y, Li L, Li Y, Wang K, Wei D, Xu S, Feng B, Che L, Fang Z, Li J, Zhuo Y, Wu D. 2019. Interpretation of fiber supplementation on offspring testicular development in a pregnant sow model from a proteomics perspective. *Int J Mol Sci* 20:4549. <https://doi.org/10.3390/ijms20184549>.
52. Datsenko KA, Wanner BL. 2000. One-step inactivation of chromosomal genes in *Escherichia coli* K-12 using PCR products. *Proc Natl Acad Sci U S A* 97:6640–6645. <https://doi.org/10.1073/pnas.120163297>.
53. Li B, Yue Y, Yuan Z, Zhang F, Li P, Song N, Lin W, Liu Y, Yang Y, Li Z, Gu L. 2017. *Salmonella* STM1697 coordinates flagella biogenesis and virulence by restricting flagellar master protein FlhD4C2 from recruiting RNA polymerase. *Nucleic Acids Res* 45:9976–9989. <https://doi.org/10.1093/nar/gkx656>.
54. Li B, Li N, Wang F, Guo L, Huang Y, Liu X, Wei T, Zhu D, Liu C, Pan H, Xu S, Wang HW, Gu L. 2012. Structural insight of a concentration-dependent mechanism by which YdiV inhibits *Escherichia coli* flagellum biogenesis and motility. *Nucleic Acids Res* 40:11073–11085. <https://doi.org/10.1093/nar/gks869>.